

## Article

# Spatio-Temporal Heterogeneity of the Ecological Environment and Its Response to Land Use Change in the Chushandian Reservoir Basin

Yichen Fang, Lianhai Cao \*, Xinyu Guo, Tong Liang, Jiyin Wang, Ning Wang and Yue Chao

College of Surveying and Geo-Informatics, North China University of Water Resources and Electric Power, Zhengzhou 450046, China; fangyichenncwu@163.com (Y.F.); 13674958092@163.com (X.G.); 201601525@stu.ncwu.edu.cn (T.L.); x202210151092@stu.ncwu.edu.cn (J.W.); z202210151106@stu.ncwu.edu.cn (N.W.); z202210151118@stu.ncwu.edu.cn (Y.C.)

\* Correspondence: caolianhai1970@163.com

**Abstract:** Conducting ecological monitoring assessments and revealing the effects of driving factors are crucial for enhancing ecological safety and promoting sustainable development. Taking the Chushandian Reservoir basin as the research object, this paper employed the Remote Sensing Ecological Index (RSEI), constructed based on remote sensing data, to monitor and assess the ecological environment of the study area from 1990 to 2021, and predicted its future development trend through the Hurst index. On this basis, we integrated land use data to elucidate the response of the ecological environment to human activities. The results show that: (1) The mutation test indicates that selecting 1990, 2004, 2008, 2013, and 2021 as the study time nodes can comprehensively reflect the spatio-temporal information regarding changes in ecological quality in the study area. Specifically, both 1990 and 2021 exhibit higher ecological quality ratings, while 2008 has the lowest ecological quality rating. The spatial distribution of ecological quality is strongly clustered, with high–high clustering and low–low clustering dominating. (2) The overall trend of ecological quality in the study area appears in a pattern of initial decline followed by subsequent improvement. From 1990 to 2004, the degraded area constituted the largest proportion, accounting for 87.82%. After 2008, the quality of the ecological environment began to rebound. Between 2008 and 2013, the proportion of regions with improved ecological conditions was 57.91%, and from 2013 to 2021, 46.74% of the regions showed improvement. (3) In the research area, 36.70% of the regions exhibit a trend of sustainable stability into the future, representing the highest proportion. Approximately 34.3% of the areas demonstrate a trend of sustainable improvement, while the regions exhibiting sustainable degradation account for only 5.72%. While the ecological environment is demonstrating a positive overall developmental trend, it is crucial to stay vigilant regarding areas of ongoing degradation and implement appropriate protective measures. (4) Land use change significantly impacts the ecological environment, with the expansion of land for urban build up causing some ecological deterioration, while the later expansion of forest improves ecological quality. The results provide theoretical approaches and a foundation for decision-making in the ecological management of the Chushandian Reservoir basin.

**Keywords:** remote sensing ecological index; ecological environment; Google Earth Engine; spatio-temporal heterogeneity; land use change; Chushandian Reservoir basin



**Citation:** Fang, Y.; Cao, L.; Guo, X.; Liang, T.; Wang, J.; Wang, N.; Chao, Y. Spatio-Temporal Heterogeneity of the Ecological Environment and Its Response to Land Use Change in the Chushandian Reservoir Basin. *Sustainability* **2024**, *16*, 1385. <https://doi.org/10.3390/su16041385>

Academic Editor: Hariklia D. Skilodimou

Received: 14 January 2024

Revised: 4 February 2024

Accepted: 5 February 2024

Published: 6 February 2024



**Copyright:** © 2024 by the authors. Licensee MDPI, Basel, Switzerland. This article is an open access article distributed under the terms and conditions of the Creative Commons Attribution (CC BY) license (<https://creativecommons.org/licenses/by/4.0/>).

## 1. Introduction

The ecological environment is inextricably linked to humanity, and a favorable ecological environment is critical for regional sustainable development [1]. As a consequence of accelerated economic progress and substantial population expansion, the ecological repercussions of human activities are becoming more prominent. The inherent conflict of global or regional ecological problems [2–4], such as soil erosion [5] and land desertification [6]. Land is the primary medium for human activities, and anthropogenic

disturbances have caused frequent changes in land use, exerting a significant impact on the ecosystem [7]. In this context, it is essential to accurately comprehend the ecological situation of a region and uncover its response to land use change, as this is a prerequisite for further development of targeted measures for the protection of the ecological environment, which is of great practical significance for the maintenance of ecological balance and sustainable development [8].

Remote sensing technology is an indispensable tool in contemporary scientific research and practice, playing a crucial role in monitoring and evaluating ecological quality due to its attributes of speed, real-time capability, and wide monitoring range [9]. Google Earth Engine (GEE) is a cloud computing platform developed by Google, widely utilized in various research fields, including surface cover and land use [10], climate and meteorological monitoring [11], ecological and environmental assessment [12], water body extraction [13–15], and urban expansion and planning [16,17]. Early studies of various ecosystems primarily relied on a single ecological index, such as the vegetation index [18], leaf area index [19], aridity index [20], and water index [21]. As scholars deepen their understanding of the formation and development of ecosystems, it is widely recognized that a single ecological factor cannot objectively and comprehensively reflect the state of the ecological environment. Meanwhile, the development of composite indices that consider multiple factors and can comprehensively reflect the complexity of environmental issues has emerged. Currently, the most widely utilized composite indices include the Environmental Vulnerability Index [22,23], the Ecological Environment Status Index [24], the Landscape Ecological Quality Index [25], and the Remote Sensing Ecological Index (RSEI) [26–28]. RSEI, proposed by Xu et al. [26], is based on remote sensing information and integrates the most intuitive indices reflecting the ecological environment, such as greenness, humidity, dryness, and heat. It can accurately monitor and evaluate a regional ecological environment, which is widely recognized and applied by scholars.

In recent years, with the deepening of the concept of ecological civilization in China, regional ecological environment issues have received great attention from scholars in geography, ecology and other related disciplines, resulting in a large number of research results, including the characteristics of spatial patterns [29], temporal changes [30], and the research on influencing factors and driving mechanisms [31], which have become an important part of revealing the pattern of change in spatio-temporal ecological environments. According to the overall progress in research, existing studies primarily concentrate on urban regions [32], with some extending to metropolitan circles [33]. However, there is a scarcity of studies investigating ecological and land use change in reservoir basins. Li et al. [34] utilized RSEI to evaluate the spatio-temporal dynamics of Luoyang city's ecological environment from 2002, and employed a geographic detector to investigate the impact of influential factors on the city's ecosystem. Zhang et al. [33] used GEE to calculate the RSEI, assessing the ecological quality of the Chang-Zhu-Tan metropolitan circle in Central China from 2000 to 2020, and then investigated the associated influencing mechanisms. The construction and annual operation of reservoirs significantly disturb the ecological environment, causing changes in river morphology, water surface area, and land cover. Consequently, reservoir basin ecosystems become relatively fragile and more sensitive to human-induced changes [35]. Therefore, it is imperative to explore the impact of land use change on the ecological quality of reservoir basins, thereby promoting the extension of ecological quality theory to them and providing guidance for ecological conservation and management. In addition, previous studies have primarily focused on ecological assessment using RSEI to uncover historical phenomena, while ignoring the prediction of future patterns. Predicting future patterns in the ecological environment is advantageous for comprehending forthcoming macro trends, and provides theoretical guidance for the development of pertinent policies.

The Chushandian Reservoir is the sole large reservoir in the upper reaches of the Huaihe River, which ranks as the fifth longest river in China. The reservoir directly impacts the ecological quality of a basin covering an area of 2900 km<sup>2</sup>, and the well-being of

1.7 million residents downstream. However, the primary focus of ecological research in the Chushandian Reservoir basin has been on the estimation of ecosystem service values [36] and the implementation of landscape ecology analysis [37]. There is insufficient research in fields such as long-term ecological monitoring and assessment, as well as the investigation of effect processes. This limitation hampers ecological conservation and the scientific formulation of governance measures. Therefore, this paper focuses on the Chushandian Reservoir basin and utilizes analytical methodologies such as RSEI, spatial autocorrelation, coefficient of variation, and the Hurst index to investigate the spatio-temporal variations in the ecological environment and explore the ecological response of land use change. This paper aimed to: (1) explore the spatio-temporal distribution characteristics of the ecological environment; (2) predict the future trend of ecological environment change; and (3) uncover the impact of land use change on the regional ecological environment.

## 2. Materials and Methods

### 2.1. Study Area

The Chushandian Reservoir basin is situated in the southern part of Henan Province, China, within the climatic zone of northern subtropical humid conditions. The annual average temperature is 15.0 °C, the annual precipitation is 1139 mm, and the annual evaporation from the water surface is about 980 mm. The reservoir basin predominantly exhibits a geomorphological structure characterized by low mountain and hill landscapes. The western and southern parts of the reservoir area feature low mountains with elevations exceeding 150 m, while the northern and eastern regions consist of hills with elevations ranging from approximately 100 to 110 m (Figure 1). The predominant vegetation consists of deciduous needle- and broad-leaved forests, with thriving pine forests in the majority of areas upstream of the reservoir displaying high vegetation coverage. Nevertheless, the vegetation is sparse in certain hilly regions. The regional ecosystem mostly comprises forests, bushes, meadows, farming, rivers, and settlements. Situated upstream of the main course of the Huaihe River and approximately 15 km from Xinyang City, the Chushandian Reservoir functions as a significant hydraulic hub primarily dedicated to flood control. It integrates irrigation, water supply, and power generation for comprehensive utilization. The basin spans an area of 2900 km<sup>2</sup>, boasting a total storage capacity of 1.25 km<sup>3</sup>. The irrigation area extends to 103.34 km<sup>2</sup>. The reservoir supplies Xinyang City with a substantial amount of water for urban living and industrial purposes. The reservoir project commenced on 16 August 2015, and reservoir impoundment began in May 2019 [36]. Conducting ecological assessment studies in the reservoir basin can provide essential data and decision support for effective environmental protection and resource management. This is critical for regional ecological environment planning and the attainment of the Sustainable Development Goals.

### 2.2. Data Sources and Pre-Processing

- (1) Remote sensing data: we used Landsat and MODIS remote sensing images with a resolution of 30 m, provided by GEE (<https://earthengine.google.com> (accessed on 25 June 2023)), incorporating both radiometric calibration and cloud removal. GEE provides extensive Earth observation data and computational resources, facilitating users in data processing and analysis. We utilized remote sensing images with prominent vegetation features taken between June and September each year for the calculation of indices.
- (2) DEM data: the DEM data used in this paper is the “ASTER Global Digital Elevation Model” with a resolution of 30 m, from the Geospatial Data Cloud (<https://www.gscloud.cn> (accessed on 25 June 2023)).
- (3) Vector data: the vector boundary data of the study area was obtained by conducting hydrological analysis on DEM data in ArcGIS.

- (4) Land use data: the land use data used in this paper is the 30 m resolution Global Land Use Dynamic Monitoring product developed by the Aerospace Information Research Institute of the Chinese Academy of Sciences [38].

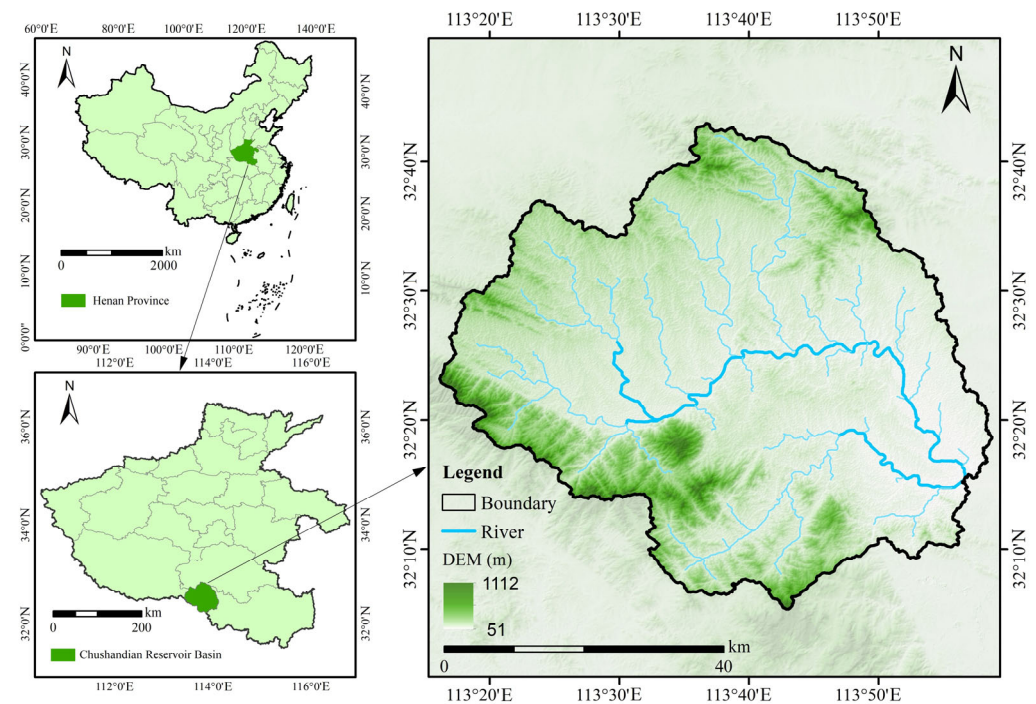


**Figure 1.** Location and topography of study area.

### 2.3. Methodology

#### 2.3.1. Research Framework

We employed remote sensing data for calculating environmental indices. The normalized difference vegetation index (NDVI) was utilized to indicate greenness, the wetness component (WET) was utilized to indicate humidity, the normalized differential building-soil index (NDBSI) was utilized to indicate dryness, and land surface temperature (LST) was utilized to indicate heat. The four indices were normalized and then underwent principal component extraction in order to create the RSEI, which was used to assess the quality of the ecological environment in the research area [39]. On this basis, we explored the impact of land use type transformation on the quality of the ecological environment by analysing land use data (Figure 2).

#### 2.3.2. Calculation of Indices

##### (1) Greenness index

NDVI is based on reflectance data from different spectral bands, reflecting the photosynthetic activity and biomass distribution of vegetation. It is commonly used to assess the greenness and growth status of vegetation [40]. The formula is as follows [41]:

$$NDVI = \frac{B_{nir} - B_{red}}{B_{nir} + B_{red}} \quad (1)$$

where  $B_{nir}$  is the reflectance in the near-infrared band of Landsat imagery data, and  $B_{red}$  is the reflectance in the red band of Landsat imagery data.

##### (2) Humidity index

The Kirchhoff transform is a data processing method used to extract specific surface information from multispectral remote sensing imageries. Applying the Kirchhoff Transform allows for the extraction of brightness, greenness, and humidity components. The

humidity component can be employed to analyze data pertaining to soil moisture and vegetation water content. The formulas used to calculate the humidity index based on Landsat imagery are as follows [42]:

$$\begin{cases} WET_{TM} = 0.0315B_{blue} + 0.2021B_{green} + 0.3012B_{red} \\ \quad + 0.1594B_{nir} - 0.6806B_{swir1} - 0.6109B_{swir2} \\ WET_{ETM} = 0.2626B_{blue} + 0.2141B_{green} + 0.0926B_{red} \\ \quad + 0.0656B_{nir} - 0.7629B_{swir1} - 0.5388B_{swir2} \\ WET_{OLI} = 0.1509B_{blue} + 0.1973B_{green} + 0.3279B_{red} \\ \quad + 0.3408B_{nir} - 0.7112B_{swir1} - 0.4572B_{swir2} \end{cases} \quad (2)$$

where  $WET_{TM}$ ,  $WET_{ETM}$ , and  $WET_{OLI}$  represent the humidity components for Landsat 5, Landsat 7, and Landsat 8, respectively.  $B_{blue}$ ,  $B_{green}$ ,  $B_{red}$ ,  $B_{nir}$ ,  $B_{swir1}$ , and  $B_{swir2}$  represent the reflectances of the blue, green, red, near-infrared, shortwave infrared 1, and shortwave infrared 2 bands in Landsat imagery, respectively.

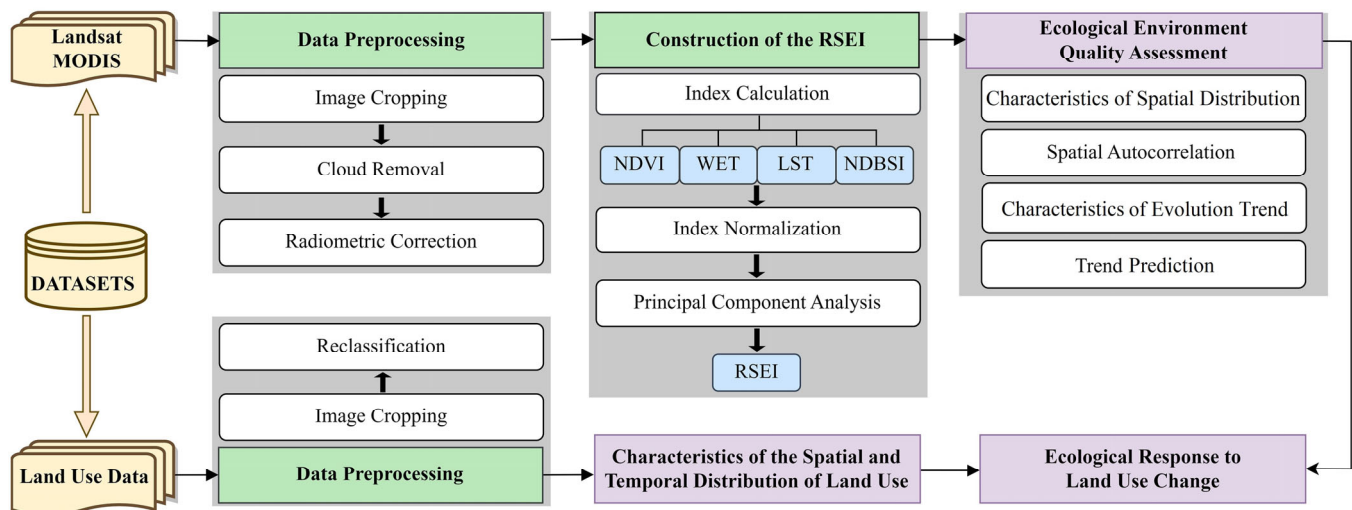


**Figure 2.** Research framework in this paper.

### (3) Dryness index

The Index-Based Built-Up Index (IBI) and the Soil Index (SI) are frequently employed to reflect land cover attributes [41]. The NDBSI, calculated as the average of IBI and SI, can reflect the influence of soil dryness and human activities on the land cover ecosystem [26]. The formulas are as follows [43]:

$$\begin{cases} NDBSI = \frac{SI+IBI}{2} \\ IBI = \frac{\left(\frac{2B_{swir1}}{B_{swir1}+B_{nir}} - \frac{B_{nir}}{B_{nir}+B_{red}} - \frac{B_{green}}{B_{green}+B_{swir1}}\right)}{\left(\frac{2B_{swir1}}{B_{swir1}+B_{nir}} + \frac{B_{nir}}{B_{nir}+B_{red}} + \frac{B_{green}}{B_{green}+B_{swir1}}\right)} \\ SI = \frac{(B_{swir1}+B_{red})-(B_{nir}+B_{blue})}{(B_{swir1}+B_{red})+(B_{nir}+B_{blue})} \end{cases} \quad (3)$$

where  $B_{blue}$ ,  $B_{green}$ ,  $B_{red}$ ,  $B_{nir}$ , and  $B_{swir1}$  represent the reflectances of the blue, green, red, near-infrared, and shortwave infrared 1 bands in Landsat imagery, respectively.

### (4) Heat index

LST reflects the state and distribution of heat at the surface and is commonly employed to investigate surface energy balance, climate change, and the urban heat island effect [44]. The formula is as follows:

$$LST = DN \times 0.02 - 273.15 \quad (4)$$

where DN represents the pixel values of the MOD11A2 imagery.

### 2.3.3. Construction of RSEI

Due to the variation in scales and value domains among the four indices, normalization is required to ensure comparability of their weights during principal component analysis. The formula is as follows [45]:

$$E_i = \frac{DN_i - DN_{i-\min}}{DN_{i-\max} - DN_{i-\min}} \quad (i = 1, 2, \dots, n) \quad (5)$$

where  $E_i$  represents the normalized index value,  $DN_i$  is the original pixel value,  $DN_{i-\min}$  is the minimum pixel value, and  $DN_{i-\max}$  is the maximum pixel value.

Principal Component Analysis (PCA) is a method used to reduce the dimensionality of data by transforming the original dataset into a new set of uncorrelated principal components. These components are subsequently arranged in descending order based on their contributions to the overall variance of the data [46]. By selecting the top few principal components, the original data is effectively reduced to a lower dimension while retaining a significant portion of the information present in the original dataset.

Conducting PCA on the four indicators through GEE yields the first principal component (PC1). To ascertain that a higher value of PC1 indicates favorable ecological circumstances, RSEI is derived by subtracting the estimated PC1 from 1. The RSEI value ranges from 0 to 1, with a higher value suggesting a superior ecological condition [26]. The formulas are as follows:

$$\begin{cases} PC1 = f(NDVI, WET, NDBSI, LST) \\ RSEI = 1 - f(NDVI, WET, NDBSI, LST) \end{cases} \quad (6)$$

Ecological quality is classified into five levels based on RSEI values with intervals of 0.2 (Table 1). The purpose is to simplify data interpretation and comparison, providing a more intuitive representation of differences in ecological conditions.

**Table 1.** Classification of ecological quality levels.

RSEI Values	Levels
$0 \leq RSEI < 0.20$	poor
$0.20 \leq RSEI < 0.40$	fair
$0.40 \leq RSEI < 0.60$	moderate
$0.60 \leq RSEI < 0.80$	good
$0.80 \leq RSEI \leq 1$	excellent

### 2.3.4. Moving T-Test

The moving  $t$ -test is a hypothesis testing method specifically tailored for time series data. Serving as an extension of the  $t$ -test, its primary purpose is to identify breakpoints within time series datasets. The paramount advantage of this method resides in its capacity to discern substantial alterations within time series patterns, thereby enabling the discernment of anomalous occurrences and shifts in states. The foundational principle of the moving  $t$ -test is that a qualitative change in averages is indicated when the difference in averages between two subsequences exceeds a predefined level of significance. The formulas are as follows [47]:

$$\begin{cases} t = \frac{\bar{X}_1 - \bar{X}_2}{S \sqrt{\frac{1}{n_1} + \frac{1}{n_2}}} \\ S = \sqrt{\frac{n_1 S_1^2 + n_2 S_2^2}{n_1 + n_2 - 2}} \end{cases} \quad (7)$$

where  $t$  is the test statistic;  $n_1$  and  $n_2$  are the sample sizes of the two subsequences;  $\bar{X}_1$  and  $\bar{X}_2$  are the means of the two subsequences; and  $S_1^2$  and  $S_2^2$  are the variances of the two subsequences.

### 2.3.5. Spatial Autocorrelation Analysis

Spatial autocorrelation analysis utilizes the global Moran's  $I$  and local Moran's  $I$  indices to reveal spatial correlations [48]. The calculation result of global Moran's  $I$  ranges between  $-1$  and  $1$ , with a larger absolute value indicating a stronger spatial autocorrelation. A positive global Moran's  $I$  value ( $I > 0$ ) signifies positive spatial autocorrelation, while a negative value ( $I < 0$ ) indicates negative spatial autocorrelation. A global Moran's  $I$  value of  $0$  denotes the absence of spatial autocorrelation. The visualization of local Moran's  $I$  is commonly achieved through the LISA cluster map, which classifies clustering as High-High, High-Low, Low-High, Low-Low, or Not significant [49]. High-High and Low-Low denote agglomeration in areas with relatively high (low) RSEI values, while High-Low and Low-High signify the coexistence of areas with high and low RSEI values, highlighting a contrasting phenomenon. "Not significant" indicates that the spatial correlation between RSEI values lacks significance in geographical space.

$$\left\{ \begin{array}{l} \text{Global Moran's } I_i = \frac{n \sum_{i=1}^n \sum_{j=1}^m W_{ij} (x_i - \bar{x})(x_j - \bar{x})}{\left( \sum_{i=1}^n \sum_{j=1}^m W_{ij} \right) \sum_{i=1}^n (x_i - \bar{x})^2} \\ \text{Local Moran's } I_i = \frac{n(x_i - \bar{x}) \sum_{j=1}^m W_{ij} (x_j - \bar{x})}{\sum_{i=1}^n (x_i - \bar{x})^2} \end{array} \right. \quad (8)$$

where  $n$  represents the number of spatial units in the study area;  $x_i$  and  $x_j$  represent the attribute values of spatial units  $i$  and  $j$ , respectively;  $\bar{x}$  represents the mean value of RSEI; and  $W_{ij}$  represents the spatial weight matrix.

### 2.3.6. Stability Analysis of Time Series

This paper employed the coefficient of variation to assess the stability of the time series, indicating the extent of variation. A larger value indicates a more dispersed distribution and lower stability in the time series. Conversely, a smaller value indicates a more concentrated distribution and higher stability over time. The formula for calculating the coefficient of variation is as follows [50]:

$$CV = \frac{\sqrt{\frac{1}{n} \sum_{i=1}^n (RSEI_i - \frac{1}{n} \sum_{i=1}^n RSEI_i)^2}}{\frac{1}{n} \sum_{i=1}^n RSEI_i} \quad (9)$$

where  $CV$  is the coefficient of variation;  $n$  is the number of years; and  $RSEI_i$  is the RSEI for each year.

To intuitively reflect the time series stability of ecological environmental changes in the study area, this paper employs the natural breaks method to categorize the coefficient of variation into five categories (Table 2). The natural breaks method aims to categorize the study subject into groups with similar characteristics by identifying the natural breakpoints within the sequences, each of which holds statistical significance.

### 2.3.7. Sustainability Analysis

Sustainability analysis predicts future changes based on existing trends. This paper conducted a sustainability analysis of the temporal changes in the ecological environment based on the Hurst index. The Hurst index, ranging from  $0$  to  $1$ , denotes the presence of

long-term memory in a time series when exceeding 0.5, which suggests a tendency for the observed trend to persist into the future [50]. This study employed rescaled range analysis (R/S) to construct the Hurst index, with the formulas as follows [51]:

$$\begin{cases} Y_t = \sum_{i=1}^t X_i \\ S_t = \sqrt{\frac{1}{t} \sum_{i=1}^t (Y_i - \bar{Y})^2} \\ R_t = \max(Y_1, Y_2, \dots, Y_t) - \min(Y_1, Y_2, \dots, Y_t) \\ \frac{R}{S} = \frac{R_t}{S_t} \\ H = \log_{\frac{1}{2}} \frac{R}{S} \end{cases} \quad (10)$$

where  $X_i$  is the original time series data point;  $R_t$  is the difference between the maximum and minimum values of the data within the window;  $S_t$  is the standard deviation of data within the window; and  $H$  is the Hurst index.

**Table 2.** Classification of temporal stability levels.

CV Value	Temporal Stability
$0 < CV \leq 0.12$	Very stable
$0.12 < CV \leq 0.17$	Relatively stable
$0.17 < CV \leq 0.22$	Slightly variable
$0.22 < CV \leq 0.34$	Moderately variable
$0.34 < CV \leq 1$	Highly variable

### 3. Results and Analysis

#### 3.1. Trend Analysis and Mutation Test of RSEI Time Series

The annual average trend of RSEI from 1990 to 2021 is shown in Figure 3a. The mean of RSEI exhibits a trend of initially decreasing and then increasing, with 2008 representing the lowest point. The average RSEI value declined from 0.84 in 1990 to 0.59 in 2008, and increased to 0.80 in 2021. The  $t$ -value of the time series exceeded the significant interval in 2004 and 2013, indicating these two years as breakpoints in the time series (Figure 3b). Consequently, we selected specific years as temporal nodes for segmenting the long time series data in the study area: 1990 (start of the study period), 2004 (breakpoint), 2008 (minimum value), 2013 (breakpoint), and 2021 (end of the study period).

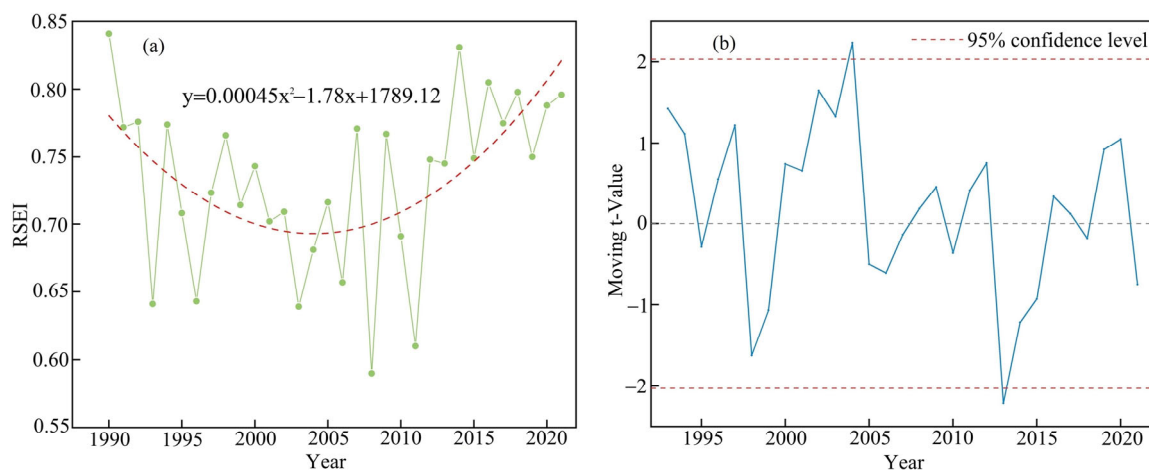


**Figure 3.** Trend and breakpoint detection of RSEI. (a) Annual mean series of RSEI. (b) Moving  $t$ -test.

### 3.2. Spatial Pattern Analysis of Ecological Environment

#### 3.2.1. Spatial Distribution of Ecological Environment

The spatial distribution of the four environmental indices in the study area exhibited significant variations (Figure 4). Higher NDVI and WET were prevalent in the low hills of both the southwestern and northern regions of the Chushandian Reservoir basin. The elevated vegetation cover in these areas indicated a positive correlation among NDVI, WET, and vegetation coverage. Conversely, the western urban areas and densely cultivated regions in the central-northern part of the study area exhibited higher values of NDBSI and LST. Influenced by urbanization and agricultural activities, these areas demonstrated heightened aridity and heat accumulation, suggesting that human activities have significantly impacted the ecological quality of the study area.

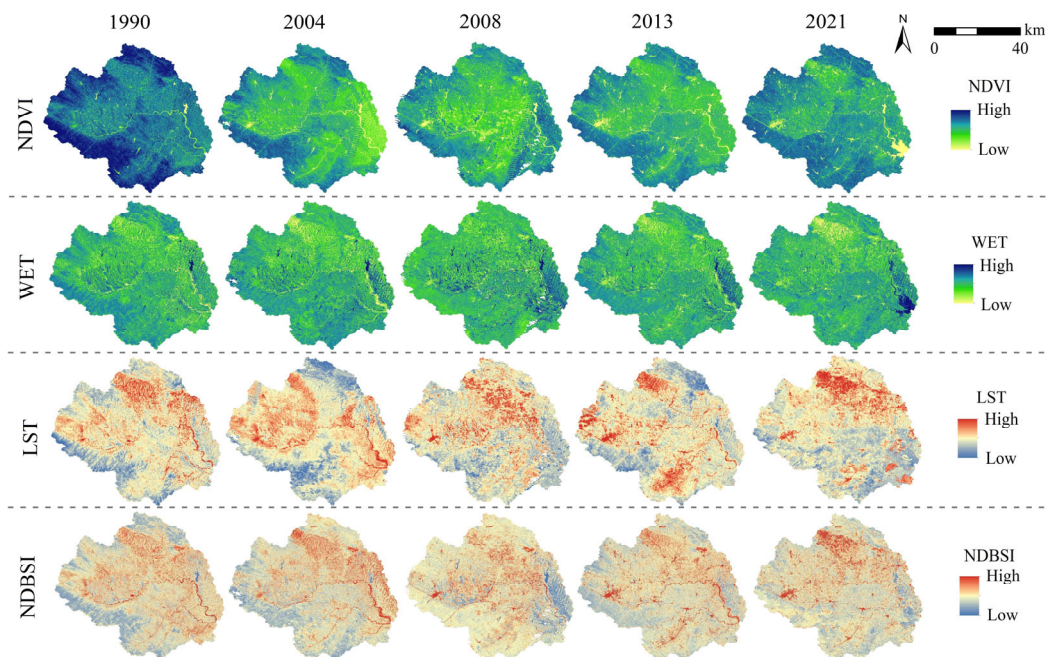


**Figure 4.** Spatial distribution of NDVI, WET, LST, and NDBSI.

We conducted a statistical analysis of the ecological quality levels in the study area (Figure 5). In 1990, regions classified as excellent covered 2346.75 km<sup>2</sup>, accounting for 80.92%, indicating superior ecological quality. In 2004, the area classified as excellent significantly decreased to 115.38 km<sup>2</sup>, representing 3.98%. In contrast, the area of the good level increased to 1838.57 km<sup>2</sup>, constituting 63.40%. By 2008, ecological quality was predominantly categorized as the moderate and good levels. The area of moderate level covered 1296.73 km<sup>2</sup>, while the area of the good spanned 1523.05 km<sup>2</sup>, making up 44.71% and 52.52% of the total area, respectively. However, the area classified as an excellent level was only 6.09 km<sup>2</sup>, accounting for merely 0.21%. After 2008, the area classified as excellent level began to steadily increase. In 2013, the area with an excellent level attained 671.15 km<sup>2</sup>, accounting for 23.14%. Concurrently, the area with a good level reached 2084.77 km<sup>2</sup>, representing the largest proportion at 71.89%. In 2021, the ecological quality was predominantly characterized by an excellent level, covering an area of 1758.16 km<sup>2</sup>, accounting for 60.63%. Additionally, the area with a good level covered 1066.72 km<sup>2</sup>, accounting for 36.78%. It is worth noting that the regions classified as “poor” in the eastern and southeastern parts, correspond to the locations of Laoyahе Reservoir and Chushandian Reservoir, respectively. The construction of these reservoirs has caused significant disturbance to the ecological environment, resulting in the conversion of forest and cropland into built-up areas and water. Consequently, this has had detrimental effects on the ecological quality within the reservoir area.

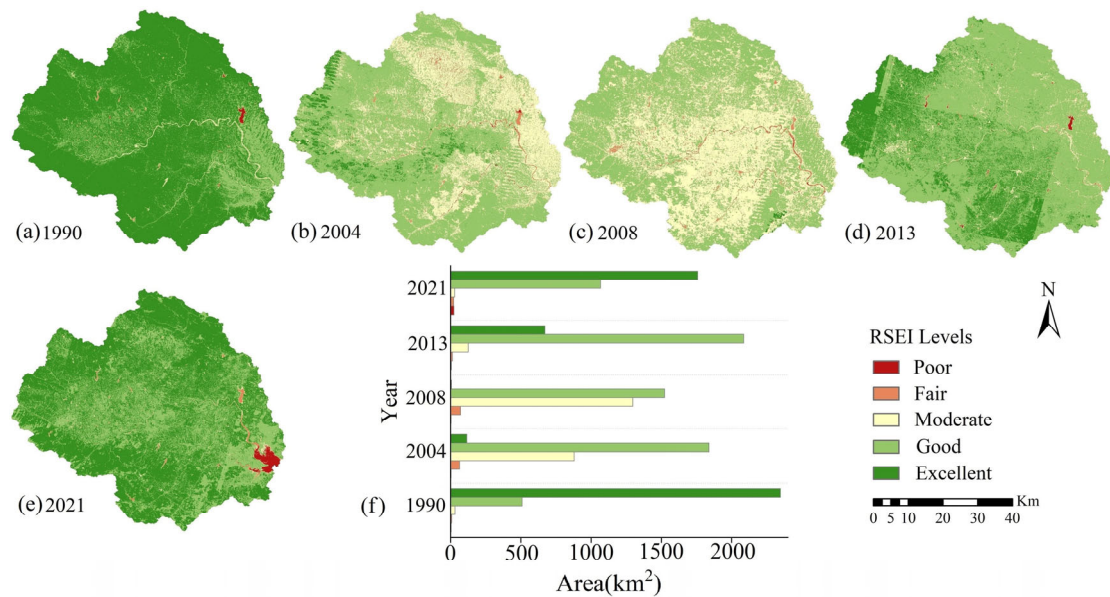


**Figure 5.** Classification results of ecological quality. (a–e) Spatial distribution of ecological quality levels in 1990, 2004, 2008, 2013, and 2021. (f) Area statistics of ecological quality levels.

### 3.2.2. Autocorrelation Analysis

The mean value of global Moran's I for the five years was 0.67, indicating a strong positive correlation. This suggests that the spatial distribution of RSEI in the study area demonstrates clustering rather than random dispersion. Local Moran's I was visualized by the LISA cluster map (Figure 6), revealing that the spatial clustering characteristics of ecological quality in the study area were dominated by High-High clustering and Low-Low clustering. The distribution of High-Low clustering and Low-High clustering appears more dispersed and less pronounced. The High-High clustering areas are predominantly situated in the mountainous and hilly terrain surrounding the study region. These areas exhibit minimal distribution fluctuations, characterized by high ecological quality and relatively minor disturbances from human activities. In contrast, the Low-Low clustering areas are mainly found in urban built-up areas, cropland, and reservoir regions. These areas face substantial disruptions from human activities, especially notable seasonal changes affecting farmland, contributing to the unstable distribution of the Low-Low clustering regions.

## 3.3. Dynamic Change of Ecological Environment

### 3.3.1. Temporal Stability Analysis of RSEI

The coefficient of variation in the research area from 1990 to 2021 was mainly concentrated between 0 and 0.3, with an average value of 0.15. The pixel count with a coefficient of variation value of 0.12 was the highest, with a frequency close to 600,000 (Figure 7a). This suggests that the RSEI values within the research area exhibit a notable concentration with moderate annual variation. The spatial distribution of the coefficient of variation (Figure 7b) indicates that very stable and relatively stable areas were primarily located in the western, northern, and southern parts of the research area. These areas are characterized by elevated mountainous terrain and experience minimal human influence. The regions with slight and moderate variability were mainly located in areas with frequent human activities. These regions were largely comprised of urban land and cropland, indicating that human activities have had a discernible impact on the ecological environment. The southeastern region of the study was characterized by high variability, precisely in the area where the Chushandian Reservoir is located. The construction of the reservoir project commenced in 2015, with impoundment beginning in 2019. This suggests that the construction of the reservoir has caused a more pronounced disturbance to the ecological environment in the surrounding area.

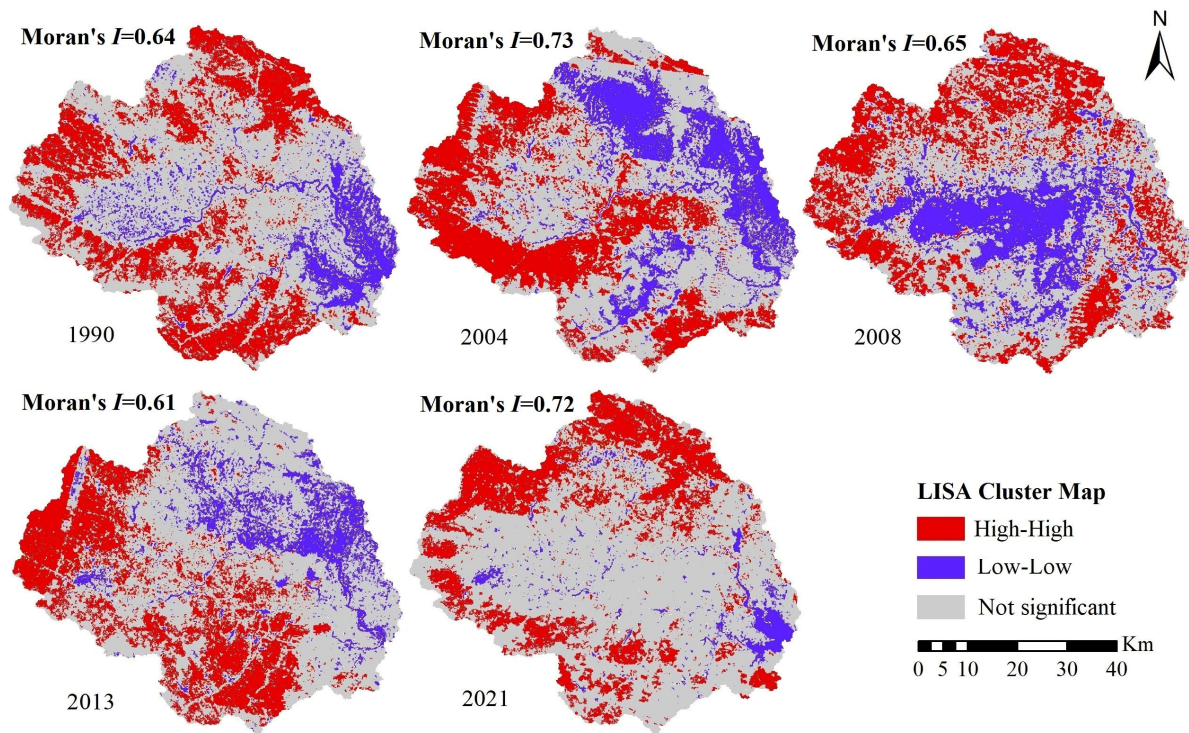


Figure 6. LISA cluster map.

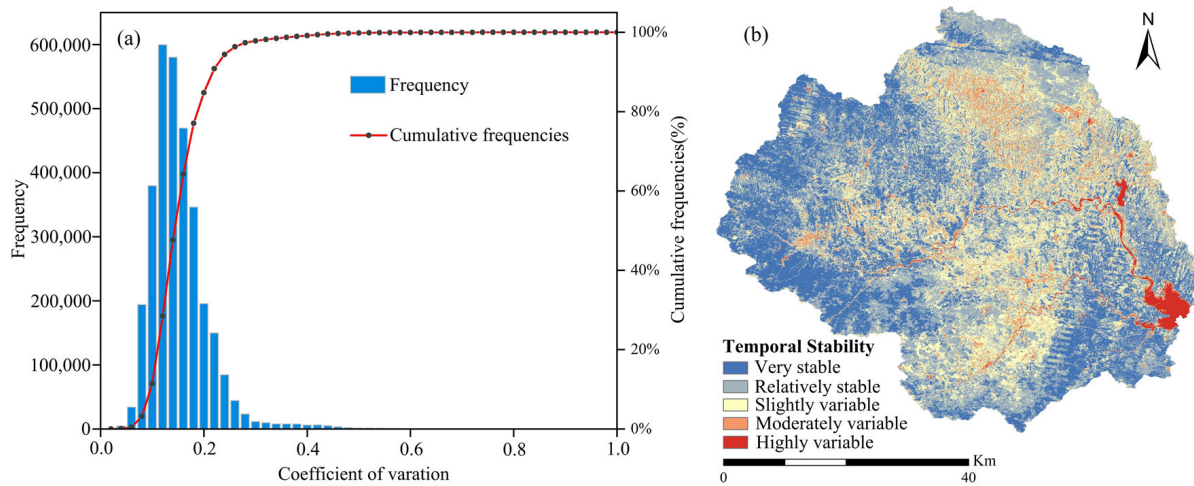
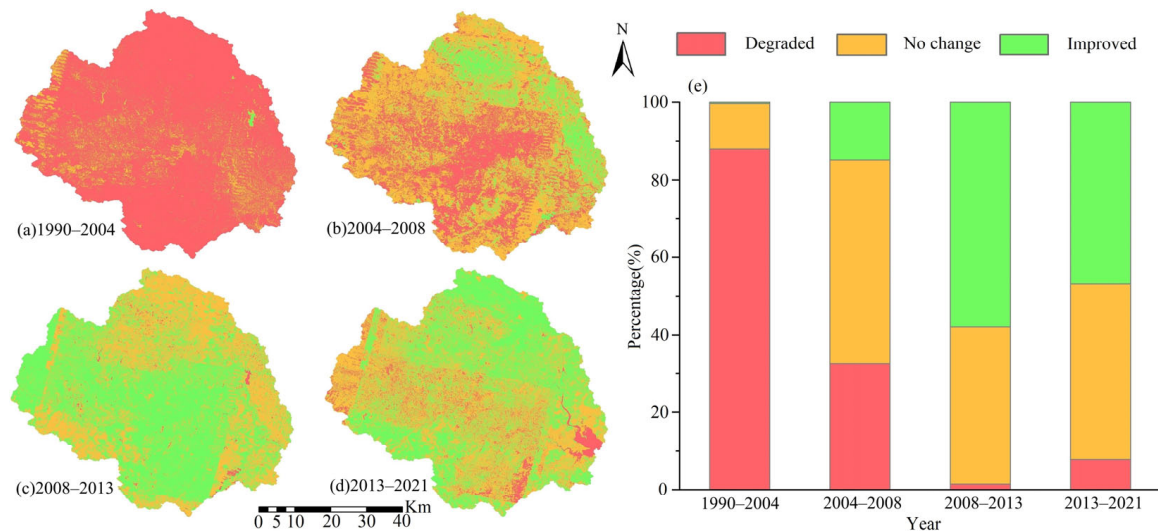


Figure 7. Classification results of temporal stability. (a) Frequency distribution of coefficient of variation. (b) Spatial distribution of temporal stability levels.

### 3.3.2. Evolution Trend of Ecological Environment

To visually represent the evolving pattern of the ecological environment in the study region, a subtraction operation was performed on the RSEI values for each year, illustrating the trend of ecological quality (Figure 8). From 1990 to 2004, there was a substantial decline in ecological quality, with an area of 2546.78 km<sup>2</sup> exhibiting a degrading trend, accounting for 87.82% of the total area. Only 0.38% of the region showed an improving trend. During this period, the ecological environment in the study area faced significant pressure. From 2004 to 2008, the degraded area amounted to 942.17 km<sup>2</sup>, constituting 32.49%, which was a significant reduction compared to the preceding period. Concurrently, the area exhibiting unchanged reached 1524.05 km<sup>2</sup>, accounting for 52.55% of the total area. This suggested a partial alleviation of the deteriorating trend in the ecological environment, with certain areas maintaining a relatively stable state. However, the proportion of areas exhibiting

improvement was only 14.96%, suggesting that there had been a limited enhancement in the overall quality of the ecological environment. During the period from 2008 to 2013, the unchanged area was 1177.05 km<sup>2</sup>, accounting for 40.59%. The improved area amounted to 1679.34 km<sup>2</sup>, representing 57.91%. This indicated a tendency for ecological quality stabilization during this period, coupled with the emergence of positive changes. From 2013 to 2021, the improved area accounted for 46.74%, highlighting the sustained trend of ecological environment improvement. Nevertheless, a minority of regions still demonstrated degradation, with a proportion of 7.15%.



**Figure 8.** Trends in ecological quality changes. (a–d) Spatial distribution of evolution types of ecological quality. (e) Proportion of area for each evolution type.

### 3.3.3. Prediction of Future Evolution Trend

This paper predicted the future trend in the ecological environment of the study area by calculating the Hurst index. The findings revealed that a substantial majority of regions in the study area, accounting for 76.71%, exhibited a Hurst index greater than 0.5. This suggested a robust inclination toward sustainability in the progression, with the potential for this trend to endure in the future. The future evolution trend of the ecological environment was derived by overlaying the Hurst index with the RSEI evolution trend (Figure 9). The region exhibiting a sustained stability trend constituted the highest proportion at 36.70%. Furthermore, areas demonstrating a sustained improvement trend accounted for 34.3%, primarily distributed in the northern and southern parts of the research area. Conversely, the area undergoing sustained degradation was minimal, comprising only 5.72% and located in the southeastern region of the study area.

Based on the analysis results, the majority of regions in the study area demonstrated a sustained stability or improvement trend, indicating a positive outlook for future development. Nevertheless, meticulous monitoring is crucial for regions exhibiting a sustained degradation trend, necessitating the implementation of appropriate protective and restoration measures.

### 3.4. Ecological Response to Land Use Change

This study reclassified land use data by consolidating second-level classifications into first-level classifications, thereby constructing spatial distribution maps of land use types in the study area over multiple years (Figure 10a). Additionally, to quantitatively depict the interconversion among different land use types, overlay analysis was conducted on land use type maps from different years, resulting in the generation of Sankey diagrams illustrating land use type transitions (Figure 10b).

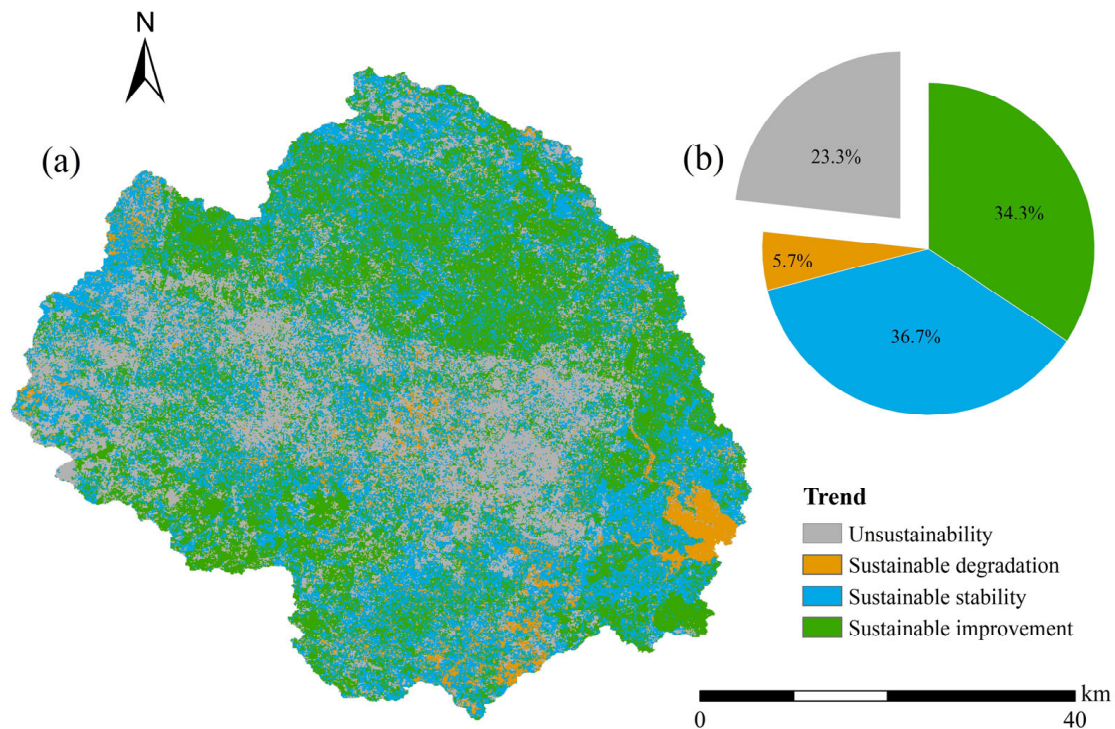


**Figure 9.** Prediction of future trends in ecological environment evolution. (a) Spatial distribution of evolution types in future. (b) Proportion of evolution types in future.

As depicted in Figure 10a, forest, cropland, and built-up are the three major land use types in the study area, collectively occupying over 95% of the total area. Forest is predominantly distributed in the low mountainous and hilly areas of the north, west, and south. Cropland is mainly distributed in the central-northern and eastern regions of the study area. Built-up is predominantly concentrated within various urban zones. It is noteworthy that the Chushandian Reservoir in the southeastern part of the study area began construction in 2015. Consequently, after 2015, the cropland and forest in the southeastern part of the study area gradually transformed into water and built-up. As depicted in Figure 10a, in 2021, a substantial area of water emerged in the reservoir area in the southeast.

As depicted in Figure 10b, there is a notable phenomenon of transformation among the three major land use types. Built-up exhibits a sustained expansion trend, with the majority of expansion areas originating from cropland and a smaller portion from forest. The extensive transformation from forest to cropland is the primary reason for the reduction in forest area. As of 2008, the total forest area had decreased by 101.03 km<sup>2</sup>. The period from 2008 to 2013 witnessed the notable success of local policies promoting the restoration of cropland to forest, leading to an increase in forest area of 82.36 km<sup>2</sup>. From 2013 to 2021, cropland and forest experienced a balanced reciprocal conversion with minimal area changes. Due to the construction and impoundment of the Chushandian Reservoir during this period, the water area increased by 17.23 km<sup>2</sup>.

In order to specifically analyze the impact of different land use types on the ecological quality of the study area, we calculated the average RSEI for each land use type (Figure 11a). Furthermore, we overlaid the RSEI of the regions where the three land use types were converted to each other to explore the driving influence of land use type conversion on the ecological quality of the environment (Figure 11b).

As depicted in Figure 11a, the RSEI of water bodies remained relatively stable, while the RSEI for the other five land use types exhibited a declining trend followed by a rising trend. The RSEI of the forest, with a multi-year average of 0.76, significantly enhanced the ecological quality in the study area. Cropland and grassland also exhibited relatively high

RSEI values, with multi-year averages of 0.71 and 0.61, respectively. In contrast, built-up, bare land, and water exhibited lower RSEI values, with multi-year averages of 0.61, 0.42, and 0.40, respectively.

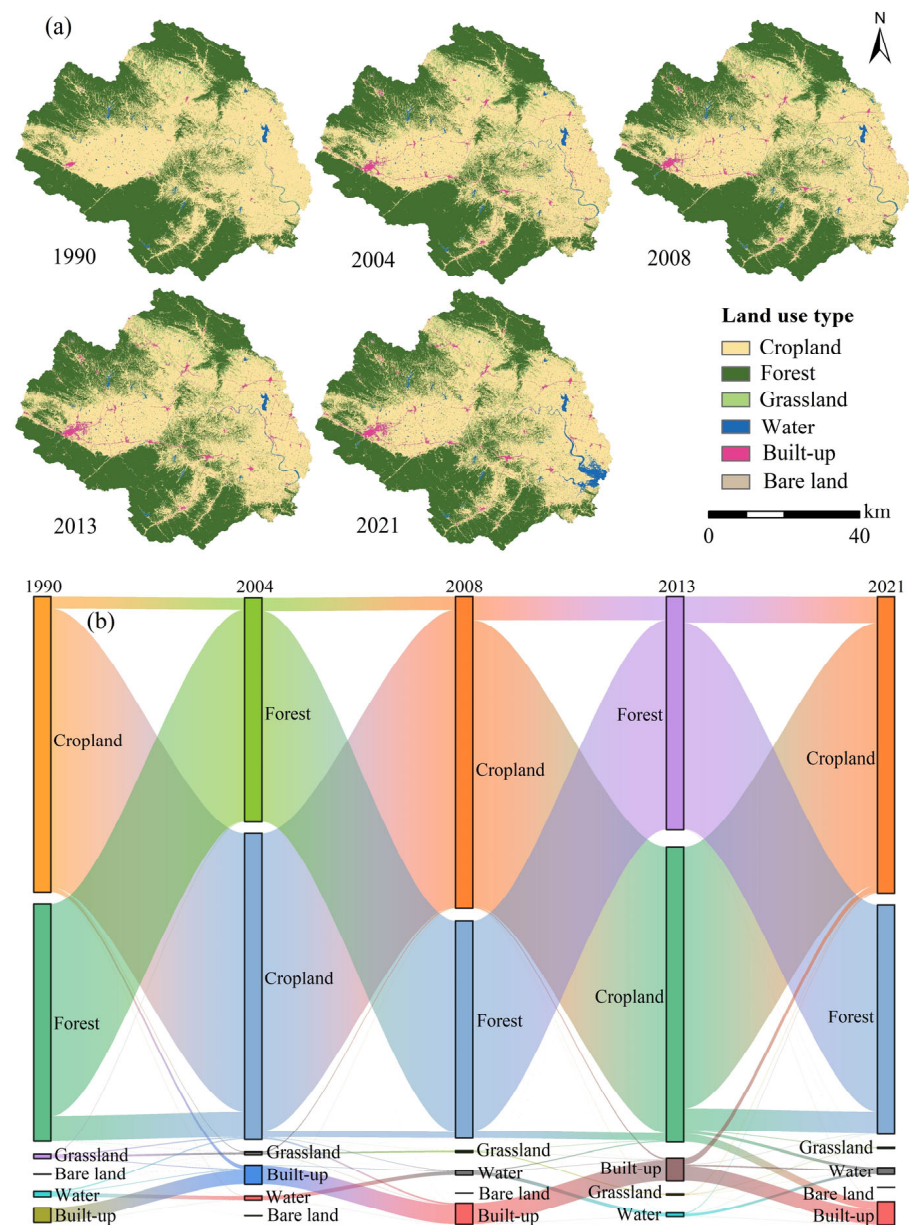


**Figure 10.** Land use characteristics in study area. (a) Land use distribution. (b) Sankey diagram of land use transition.

As depicted in Figure 11b, the regions undergoing the conversion from cropland and forest to built-up exhibited significant fluctuations in ecological quality, characterized by substantial and negative growth in RSEI. This indicates that the expansion of built-up land has a significant adverse impact on the ecological quality of the study area. The ecological degradation in areas undergoing the conversion from forest to cropland exhibited a slowing trend, with the average RSEI changing from  $-0.21$  to  $-0.09$ . The ecological quality fluctuations resulting from the restoration of cropland to forest exhibited slight changes. During the period from 2008 to 2013, the average RSEI change related to this restoration reached its maximum at 0.18, significantly enhancing the ecological quality in the study area.

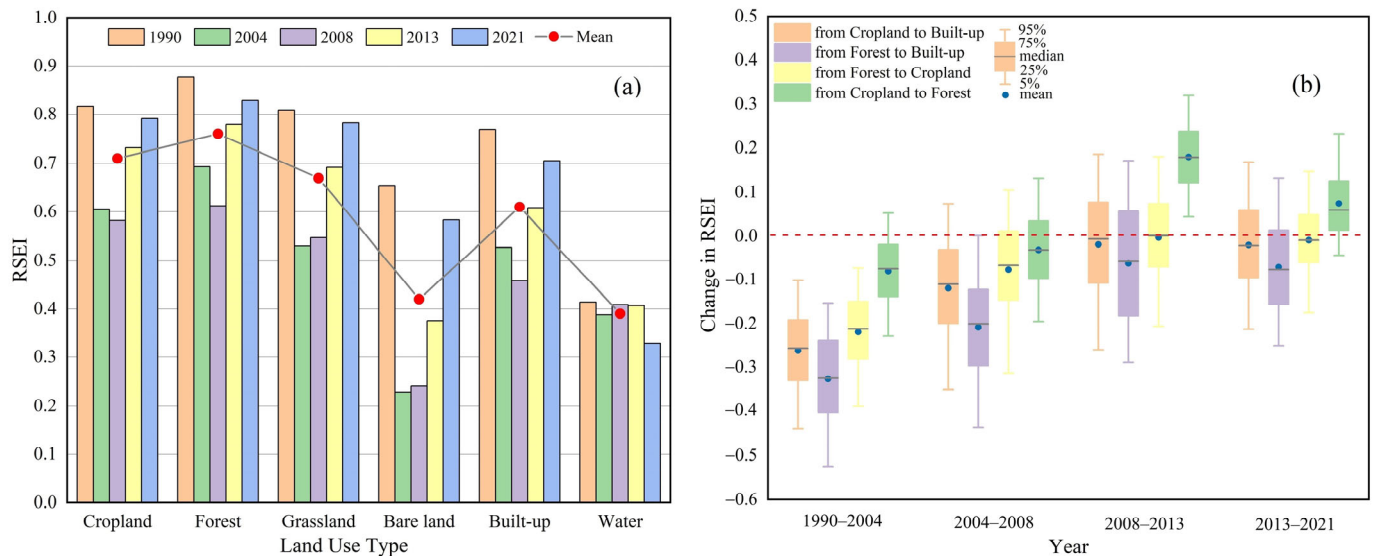


**Figure 11.** Ecological response to land use change. (a) RSEI values for different land use types. (b) RSEI change in regions undergoing land use transitions.

## 4. Discussion

### 4.1. Rationality Analysis of Ecological Assessment Results

This paper employs the method of principal component analysis, utilizing four indicators—NDVI, WET, NDBSI, and LST—to construct RSEI. A comprehensive long-term monitoring spanning 32 years was conducted (Table 3). The outcomes reveal that the contribution rates of PC1 consistently surpass 90%, signifying that PC1 encapsulates the majority of characteristic information from the original indicators [48]. This substantiates the effectiveness of principal component analysis and affirms the feasibility of representing RSEI through PC1. The loading values of NDVI and WET are positive, exhibiting a positive correlation with RSEI, indicating their beneficial impact on the ecological quality of the study area. The absolute value of NDVI loading is maximal, signifying that NDVI contributes significantly to PC1, playing a predominant role in the variation of RSEI. In contrast, the loading values of LST and NDBSI are negative, displaying a negative correlation with RSEI, suggesting their adverse impact on the ecological quality of the study area [32].

### 4.2. Impact of Human Activities on Ecological Environment

We initiated our exploration through the lens of land use transformation, delving into the impact of human activities on the quality of the ecological environment. According to our research, from 1990 to 2021, the urbanization process in the Chushandian Reservoir basin rapidly progressed, leading to an increase in the built-up area by 46.73 km<sup>2</sup>. Combining the spatial distribution of the coefficient of variation (Figure 7), we observe a pronounced disturbance in the time series of ecological quality in areas strongly coinciding with urbanization expansion. This indicates that human activities have significantly impacted the ecological quality in this region. Noteworthy is the fact that, despite the environmental degradation resulting from urban expansion, the mean RSEI of developed land stands at around 0.61, indicating a level above moderate [52]. Especially striking is the ongoing enhancement in the city's ecological quality since 2008, underscoring a shift in developmental paradigms where urban planning increasingly emphasizes ecological environment construction [53].

The implementation of policies is closely associated with changes in the ecological environment. The research findings reveal that forested is the land use type with the highest mean RSEI (Figure 11a). In 2002, the Chinese government comprehensively implemented the policy of restoring cropland to forest; prior to this, there was a drastic reduction in the area of forested land in the study area, leading to the rapid deterioration of the ecological

environment. Around 2013, the local initiatives for the restoration of cropland to forest began to yield significant results [54]. The area of forested land increased, stemming the trend of ecological degradation, and the ecological quality started to steadily improve. In 2010, the Chinese government revised the “Law of The People’s Republic of China on Water and Soil Conservation”, and Henan Province initiated extensive soil and water conservation engineering projects [55], further enhancing the local vegetation coverage. In 2016, the Chinese government introduced the “Thirteenth Five-Year Plan,” aiming to vigorously advance the construction of ecological civilization and enhance ecological functions. The implementation of these policies has had a positive impact on improving the ecological environment.

**Table 3.** Loading values of indices and the contribution of PC1.

Year	WET	NDVI	LST	NDBSI	Contribution
1990	0.51	0.68	−0.28	−0.44	96.53%
1991	0.51	0.63	−0.40	−0.44	97.13%
1992	0.58	0.52	−0.56	−0.27	98.48%
1993	0.52	0.63	−0.38	−0.44	96.34%
1994	0.51	0.66	−0.38	−0.39	96.91%
1995	0.52	0.61	−0.43	−0.41	95.20%
1996	0.53	0.63	−0.31	−0.48	97.18%
1997	0.51	0.60	−0.43	−0.45	94.96%
1998	0.59	0.56	−0.36	−0.45	96.34%
1999	0.49	0.60	−0.39	−0.49	97.07%
2000	0.54	0.65	−0.31	−0.42	96.80%
2001	0.58	0.65	−0.05	−0.49	96.12%
2002	0.52	0.51	−0.43	−0.53	98.49%
2003	0.56	0.63	−0.41	−0.36	97.83%
2004	0.60	0.68	−0.36	−0.19	98.39%
2005	0.59	0.57	−0.29	−0.50	97.73%
2006	0.58	0.64	−0.26	−0.43	96.08%
2007	0.68	0.43	−0.50	−0.33	96.65%
2008	0.63	0.66	−0.34	−0.23	98.55%
2009	0.50	0.59	−0.32	−0.54	99.19%
2010	0.52	0.51	−0.43	−0.54	99.25%
2011	0.64	0.56	−0.37	−0.38	96.90%
2012	0.62	0.57	−0.37	−0.40	97.94%
2013	0.54	0.70	−0.30	−0.37	97.73%
2014	0.58	0.64	−0.35	−0.36	98.01%
2015	0.53	0.61	−0.44	−0.40	97.89%
2016	0.53	0.68	−0.40	−0.31	98.06%
2017	0.53	0.63	−0.46	−0.34	97.98%
2018	0.55	0.66	−0.35	−0.37	97.92%
2019	0.57	0.66	−0.34	−0.34	97.14%
2020	0.50	0.66	−0.40	−0.38	98.14%
2021	0.54	0.67	−0.34	−0.38	97.31%

#### 4.3. Limitations and Future Work

Primarily, constrained by spatial resolution and quality, there exists a certain disparity between the information contained in remote sensing imagery and the actual information, preventing a detailed characterization of environmental information [50]. This discrepancy leads to errors in computing indicators and constructing RSEI. However, the research results still indicate the effectiveness of this method for ecological quality assessment [33]. In subsequent studies, we plan to employ high-resolution remote sensing imagery for a more refined analysis and assessment of the ecological quality in the study area. Moreover, the construction of RSEI is highly flexible, allowing for improvements based on the specific conditions of the study area. Therefore, in future research, we will no longer be confined to the four indicators of NDVI, WET, NDBSI, and LST. Instead, we will consider the

incorporation of new indicators, such as soil erosion intensity [56], air quality [30], etc., to construct an RSEI more tailored to the characteristics of the study area, and thereby obtain more accurate results. Lastly, in terms of factor exploration, this paper focuses on analyzing the impact of human activities on the ecological environment of the study area. In reality, the ecological environment is influenced by both human activities and natural factors. Future research will incorporate natural factors such as topography, climate, rainfall, etc., to comprehensively explore the influencing factors on ecological quality.

## 5. Conclusions

This paper utilized remote sensing data provided by GEE to monitor and assess the ecological environment of the Chushandian Reservoir basin through the construction of RSEI. Additionally, in conjunction with land use data, we analyzed the impact of land use type conversion on the ecological quality. The research outcomes possess certain reference value and application potential. The main conclusions are as follows:

- (1) The ecological quality levels of the Chushandian Reservoir basin were predominantly excellent in 1990 and 2021. In 2004 and 2008, lower RSEI values indicated extensive areas with a moderate level, while areas classified as good were widely distributed in each respective year. The spatial distribution of ecological quality in the study area exhibits strong clustering, with high-high and low-low clustering being the predominant clustering features.
- (2) The proportion of areas experiencing ecological degradation was as high as 87.82% from 1990 to 2004. Between 2004 and 2008, 32.49% of the regions demonstrated degradation. However, after 2008, the ecological quality started to rebound. The proportion of areas showing ecological improvement was 57.91% from 2008 to 2013, and from 2013 to 2021, 46.74% of the regions witnessed improvement.
- (3) According to the calculation results of the Hurst index, the majority of the study area exhibits a trend of sustainable stability or improvement into the future. Given the significant disturbance caused by the construction of the reservoir to the surrounding ecological environment, corresponding ecological restoration measures should be taken in the future.
- (4) Land use change has significantly influenced the ecological quality of the study area, with urban expansion leading to the deterioration of the regional ecological environment. Forest stands out as the land use type with the highest RSEI, and the implementation of policies such as the restoration of cropland to forest has contributed to the improvement of the ecological environment.

**Author Contributions:** Conceptualization, L.C. and Y.F.; methodology, Y.F.; software, X.G.; validation, L.C.; formal analysis, Y.F. and Y.C.; investigation, L.C.; resources, L.C.; data curation, Y.F. and N.W.; writing—original draft preparation, Y.F.; writing—review and editing, L.C.; visualization, T.L. and J.W.; supervision, L.C.; project administration, L.C.; funding acquisition, L.C. All authors have read and agreed to the published version of the manuscript.

**Funding:** This work was supported by the National Natural Science Foundation of China (Grant No. 41971241).

**Institutional Review Board Statement:** Not applicable.

**Informed Consent Statement:** Not applicable.

**Data Availability Statement:** Landsat and MODIS products in the article are available at <https://earthengine.google.com>, accessed on 25 June 2023. DEM data in the article are available at <https://www.gscloud.cn>, accessed on 25 June 2023. Land use data in the article are available at <https://zenodo.org>, accessed on 25 June 2023.

**Conflicts of Interest:** The authors declare no conflicts of interest.

## References

1. Fischer, J.; Gardner, T.A.; Bennett, E.M.; Balvanera, P.; Biggs, R.; Carpenter, S.; Daw, T.; Folke, C.; Hill, R.; Hughes, T.P.; et al. Advancing sustainability through mainstreaming a social-ecological systems perspective. *Curr. Opin. Environ. Sustain.* **2015**, *14*, 144–149. [\[CrossRef\]](#)
2. Nathaniel, S.P.; Adeleye, N. Environmental preservation amidst carbon emissions, energy consumption, and urbanization in selected African countries: Implication for sustainability. *J. Clean. Prod.* **2021**, *285*, 125409. [\[CrossRef\]](#)
3. Khan, I.; Hou, F.; Le, H.P. The impact of natural resources, energy consumption, and pollution growth on environmental quality: Fresh evidence from the United States of America. *Sci. Total Environ.* **2021**, *754*, 142222. [\[CrossRef\]](#) [\[PubMed\]](#)
4. Speidel, J.J.; Weiss, D.C.; Ethelston, S.A.; Gilbert, S.M. Population Policies, Programmes and the Environment. *Philos. Trans. R. Soc. B Biol. Sci.* **2009**, *364*, 3049–3065. [\[CrossRef\]](#) [\[PubMed\]](#)
5. Borrelli, P.; Robinson, D.A.; Fleischer, L.R.; Lugato, E.; Ballabio, C.; Alewell, C.; Meusburger, K.; Modugno, S.; Schütt, B.; Ferro, V.; et al. An assessment of the global impact of 21st century land use change on soil erosion. *Nat. Commun.* **2017**, *8*, 2013. [\[CrossRef\]](#) [\[PubMed\]](#)
6. Sterk, G.; Stoorvogel, J. Desertification—scientific versus political realities. *Land* **2020**, *9*, 156. [\[CrossRef\]](#)
7. Jiang, W.; Fu, B.; Lü, Y. Assessing impacts of land use/land cover conversion on changes in ecosystem services value on the Loess Plateau, China. *Sustainability* **2020**, *12*, 7128. [\[CrossRef\]](#)
8. Cheng, L.; Wang, Z.; Tian, S.; Liu, Y.; Sun, M.; Yang, Y. Evaluation of eco-environmental quality in Mentougou District of Beijing based on improved remote sensing ecological index. *Chin. J. Ecol.* **2021**, *40*, 1177. (In Chinese)
9. Zhang, M.; Wang, J.; Zhang, Y.; Wang, J. Ecological response of land use change in a large opencast coal mine area of China. *Resour. Policy* **2023**, *82*, 103551. [\[CrossRef\]](#)
10. Xie, S.; Liu, L.; Zhang, X.; Yang, J.; Chen, X.; Gao, Y. Automatic land-cover mapping using landsat time-series data based on google earth engine. *Remote Sens.* **2019**, *11*, 3023. [\[CrossRef\]](#)
11. Jia, H.; Yan, C.; Xing, X. Evaluation of eco-environmental quality in Qaidam basin based on the ecological index (MRSEI) and GEE. *Remote Sens.* **2021**, *13*, 4543. [\[CrossRef\]](#)
12. Chen, W.; Huang, H.; Tian, Y.; Du, Y. Monitoring and assessment of the eco-environment quality in the Sanjiangyuan region based on Google Earth Engine. *J. Geo-Inf. Sci.* **2019**, *21*, 1382–1391. (In Chinese)
13. Liu, Y.; Tian, T.; Zeng, P.; Zhang, X.; Che, Y. Surface water change characteristics of Taihu Lake from 1984–2018 based on Google Earth Engine. *J. Appl. Ecol.* **2020**, *31*, 3163–3172.
14. Nguyen, U.; Pham, L.; Dang, T. An automatic water detection approach using Landsat 8 OLI and Google Earth Engine cloud computing to map lakes and reservoirs in New Zealand. *Environ. Monit. Assess.* **2019**, *191*, 235. [\[CrossRef\]](#)
15. Feng, K.; Mao, D.; Wang, Z.; Pu, H.; Du, B.; Qiu, Z. Spatial and temporal characteristics of water bodies occupied by global urban land expansion from 1986 to 2015 based on GEE and remote sensing big data. *Sci. Geogr. Sin.* **2022**, *42*, 143–151.
16. Xue, M.; Zhang, X.; Sun, X.; Sun, T.; Yang, Y. Expansion and evolution of a typical resource-based mining city in transition using the google earth engine: A case study of datong, China. *Remote Sens.* **2021**, *13*, 4045. [\[CrossRef\]](#)
17. Dai, S.; Yi, X.; Luo, H.; Li, H.; Li, M.; Zheng, Q.; Hu, Y. Mapping Land Use in Hainan Island Based on Google Earth Engine and Landsat Time Series Data. *Chin. J. Trop. Crops.* **2021**, *42*, 3351–3357.
18. Motohka, T.; Nasahara, K.N.; Oguma, H.; Tsuchida, S. Applicability of green-red vegetation index for remote sensing of vegetation phenology. *Remote Sens.* **2010**, *2*, 2369–2387. [\[CrossRef\]](#)
19. Hu, Y.; Li, H.; Wu, D.; Chen, W.; Zhao, X.; Hou, M.; Zhu, Y. LAI-indicated vegetation dynamic in ecologically fragile region: A case study in the Three-North Shelter Forest program region of China. *Ecol. Indic.* **2021**, *120*, 106932. [\[CrossRef\]](#)
20. Greve, P.; Roderick, M.; Ukkola, A.; Wada, Y. The aridity index under global warming. *Environ. Res. Lett.* **2019**, *14*, 124006. [\[CrossRef\]](#)
21. Gao, B. NDWI—A normalized difference water index for remote sensing of vegetation liquid water from space. *Remote Sens. Environ.* **1996**, *58*, 257–266. [\[CrossRef\]](#)
22. Wang, X.; Zhong, X.; Liu, S.; Liu, J.; Wang, Z.; Li, M. Regional assessment of environmental vulnerability in the Tibetan Plateau: Development and application of a new method. *J. Arid. Environ.* **2008**, *72*, 1929–1939. [\[CrossRef\]](#)
23. Li, A.; Wang, A.; Liang, S.; Zhou, W. Eco-environmental vulnerability evaluation in mountainous region using remote sensing and GIS—A case study in the upper reaches of Minjiang River, China. *Ecol. Model.* **2006**, *192*, 175–187. [\[CrossRef\]](#)
24. Wang, C.; Zhao, H. The assessment of urban ecological environment in watershed scale. *Procedia Environ. Sci.* **2016**, *36*, 169–175. [\[CrossRef\]](#)
25. Xu, J.; Li, G.; Chen, G.; Zhao, H.; Qu, J. Changes of landscape ecological quality for land reclamation in mining area. *Trans. Chin. Soc. Agric. Eng.* **2013**, *29*, 232–239. (In Chinese)
26. Xu, H. A remote sensing index for assessment of regional ecological changes. *China Environ. Sci.* **2013**, *33*, 889–897. (In Chinese)
27. Shan, W.; Jin, X.; Ren, J.; Wang, J.; Xu, Z.; Fan, Y.; Zhou, Y. Ecological environment quality assessment based on remote sensing data for land consolidation. *J. Clean. Prod.* **2019**, *239*, 118126. [\[CrossRef\]](#)
28. Jing, Y.; Zhang, F.; He, Y.; Johnson, V.; Arikena, M. Assessment of spatial and temporal variation of ecological environment quality in Ebinur Lake Wetland National Nature Reserve, Xinjiang, China. *Ecol. Indic.* **2020**, *110*, 105874. [\[CrossRef\]](#)
29. Sun, C.; Li, J.; Liu, Y.; Cao, L.; Zheng, J.; Yang, Z.; Li, Y. Ecological quality assessment and monitoring using a time-series remote sensing-based ecological index (ts-RSEI). *GISci. Remote Sens.* **2022**, *59*, 1793–1816. [\[CrossRef\]](#)
30. Mao, S.; She, J.; Zhang, Y. Spatial-Temporal Evolution of Land Use Change and Eco-Environmental Effects in the Chang-Zhu-Tan Core Area. *Sustainability* **2023**, *15*, 7581. [\[CrossRef\]](#)

31. Liu, P.; Ren, C.; Yu, W.; Ren, H.; Xia, C. Exploring the ecological quality and its drivers based on annual remote sensing ecological index and multisource data in Northeast China. *Ecol. Indic.* **2023**, *154*, 110589. [[CrossRef](#)]
32. Zhu, D.; Chen, T.; Wang, Z.; Niu, R. Detecting ecological spatial-temporal changes by Remote Sensing Ecological Index with local adaptability. *J. Environ. Manag.* **2021**, *299*, 113655. [[CrossRef](#)] [[PubMed](#)]
33. Zhang, Y.; She, J.; Long, X.; Zhang, M. Spatio-temporal evolution and driving factors of eco-environmental quality based on RSEI in Chang-Zhu-Tan metropolitan circle, central China. *Ecol. Indic.* **2022**, *144*, 109436. [[CrossRef](#)]
34. Li, H.; Jing, H.; Yan, G.; Guo, H.; Luan, W. Long-Term Ecological Environment Quality Evaluation and Its Driving Mechanism in Luoyang City. *Sustainability* **2023**, *15*, 11866. [[CrossRef](#)]
35. Simoes, N.; Nunes, A.; Dias, J.; Lansac-Tôha, F.; Velho, L.; Bonecker, C. Impact of reservoirs on zooplankton diversity and implications for the conservation of natural aquatic environments. *Hydrobiologia* **2015**, *758*, 3–17. [[CrossRef](#)]
36. Zhang, L.; Yang, S.; He, H.; Zhang, J.; Zhou, S.; Zhang, F.; Wu, Q. Estimation of Ecological Service Value of Soil and Water Conservation in Reservoir Engineering Area. *Yellow River* **2020**, *42*, 78–81. (In Chinese)
37. Yang, S.; Liu, J.; Wu, Q.; He, H.; Yang, F.; Li, B.; Li, P. Model and application of elastic landscape function in soil water conservation. *Yellow River* **2020**, *42*, 74–77. (In Chinese)
38. Zhang, X.; Liu, L.; Chen, X.; Gao, Y.; Xie, S.; Mi, J. GLC\_FCS30: Global land-cover product with fine classification system at 30 m using time-series Landsat imagery. *Earth Syst. Sci. Data* **2021**, *13*, 2753–2776. [[CrossRef](#)]
39. Xu, D.; Yang, F.; Yu, L.; Zhou, Y.; Li, H.; Ma, J.; Cheng, J. Quantization of the coupling mechanism between eco-environmental quality and urbanization from multisource remote sensing data. *J. Clean. Prod.* **2021**, *321*, 128948. [[CrossRef](#)]
40. Zheng, L.; Wu, M.; Zhou, M.; Zhao, L. Spatiotemporal distribution and influencing factors of *Ulva prolifera* and *Sargassum* and their coexistence in the South Yellow Sea, China. *J. Oceanol. Limnol.* **2022**, *40*, 1070–1084. [[CrossRef](#)]
41. Liu, Q.; Yu, F.; Mu, X. Evaluation of the Ecological Environment Quality of the Kuye River Source Basin Using the Remote Sensing Ecological Index. *Int. J. Environ. Res. Public Health* **2022**, *19*, 12500. [[CrossRef](#)] [[PubMed](#)]
42. Ma, D.; Huang, Q.; Liu, B.; Zhang, Q. Analysis and Dynamic Evaluation of Eco-Environmental Quality in the Yellow River Delta from 2000 to 2020. *Sustainability* **2023**, *15*, 7835. [[CrossRef](#)]
43. Zhang, P.; Chen, X.; Ren, Y.; Lu, S.; Song, D.; Wang, Y. A Novel Mine-Specific Eco-Environment Index (MSEEI) for Mine Ecological Environment Monitoring Using Landsat Imagery. *Remote Sens.* **2023**, *15*, 933. [[CrossRef](#)]
44. Willis, K. Remote sensing change detection for ecological monitoring in United States protected areas. *Biol. Conserv.* **2015**, *182*, 233–242. [[CrossRef](#)]
45. Song, W.; Gu, H.; Song, W.; Li, F.; Cheng, S.; Zhang, Y.; Ai, J. Environmental assessments in dense mining areas using remote sensing information over Qian'an and Qianxi regions China. *Ecol. Indic.* **2023**, *146*, 109814. [[CrossRef](#)]
46. Cao, S.; Chen, S. Analysis of quality evolution of important ecological function areas and implementation effects of the ecological redline in Jiangsu Province, China. *Acta Ecol. Sin.* **2023**, *43*, 8933–8947. (In Chinese)
47. Liang, L.; Li, L.; Liu, Q. Temporal variation of reference evapotranspiration during 1961–2005 in the Taoer River basin of Northeast China. *Agric. For. Meteorol.* **2010**, *150*, 298–306. [[CrossRef](#)]
48. Shan, Y.; Dai, X.; Li, W.; Yang, Z.; Wang, Y.; Qu, G.; Zeng, B. Detecting spatial-temporal changes of urban environment quality by remote sensing-based ecological indices: A case study in Panzhihua city, Sichuan Province, China. *Remote Sens.* **2022**, *14*, 4137. [[CrossRef](#)]
49. Nie, X.; Hu, Z.; Zhu, Q.; Ruan, M. Research on temporal and spatial resolution and the driving forces of ecological environment quality in coal mining areas considering topographic correction. *Remote Sens.* **2021**, *13*, 2815. [[CrossRef](#)]
50. Chen, C.; Wang, L.; Yang, G.; Sun, W.; Song, Y. Mapping of ecological environment based on Google earth engine cloud computing platform and landsat long-term data: A case study of the Zhoushan Archipelago. *Remote Sens.* **2023**, *15*, 4072. [[CrossRef](#)]
51. Chen, H.; Chen, C.; Zhang, Z.; Lu, C.; Wang, L.; He, X.; Chen, J. Changes of the spatial and temporal characteristics of land-use landscape patterns using multi-temporal Landsat satellite data: A case study of Zhoushan Island, China. *Ocean Coastal Manag.* **2021**, *213*, 105842. [[CrossRef](#)]
52. Yang, Z.; Sun, C.; Ye, J.; Gan, C.; Li, Y.; Wang, L.; Chen, Y. Spatio-temporal heterogeneity of ecological quality in Hangzhou greater bay area (HGBA) of china and response to land use and cover change. *Remote Sens.* **2022**, *14*, 5613. [[CrossRef](#)]
53. Shen, Q.; Peng, S.; Ci, h. Evolution and future prospect of urban ecological planning in modern China. *Urban Plan. Int.* **2019**, *34*, 37–48. (In Chinese) [[CrossRef](#)]
54. Zhao, B.; Liu, D. Potential impacts of multi-scenario farmland reforestation on the biodiversity conservation values of forests. *Trans. Chin. Soc. Agric. Eng.* **2022**, *38*, 239–249. (In Chinese)
55. Zhao, C.; Zhang, N.; Zhang, H.; Du, C.; Zhang, C.; Yuan, L. Distribution characteristic and counter measures of soil and water loss in Huaihe River basin. *Soil Water Conserv. China* **2022**, *12*, 15–17. (In Chinese)
56. Xu, F.; Li, H.; Li, Y. Ecological environment quality evaluation and evolution analysis of a rare earth mining area under different disturbance conditions. *Environ. Geochem. Health* **2021**, *43*, 2243–2256. [[CrossRef](#)]

**Disclaimer/Publisher's Note:** The statements, opinions and data contained in all publications are solely those of the individual author(s) and contributor(s) and not of MDPI and/or the editor(s). MDPI and/or the editor(s) disclaim responsibility for any injury to people or property resulting from any ideas, methods, instructions or products referred to in the content.